Modeling the removal of Reactive Red 120 dye from aqueous effluents by activated carbon

Kods Oueslati, Eder C. Lima, Fakher Ayachi, Mariene R. Cunha and Abdelmottaleb Ben Lamine

ABSTRACT

The adsorption isotherms of Reactive Red 120 (RR-120) on Brazilian pine-fruit shell activated carbon, at six temperatures (298, 303, 308, 313, 318 and 323 K) and pH = 6, were determined and interpreted using a double layer model with one energy. A statistical physics treatment established the formulation of this model. Steric and energetic parameters related to the adsorption process, such as the number of adsorbed molecules per site, the receptor sites density and the concentration at half-saturation, have been considered. Thermodynamic potential functions such as entropy, internal energy and Gibbs free enthalpy are analyzed, and the choice of the models is based on assumptions in correlation with experimental conditions. By numerical fitting, the investigated parameters were deduced. The theoretical expressions provide a good understanding and interpretation of the adsorption isotherms at the microscopic level. We believe that our work contributes to new theoretical insights on the dye adsorption in order to know the physical nature of the adsorption process.

Key words | adsorption isotherms, double layer model with one energy, Reactive Red 120

Kods Oueslati (corresponding author)
Fakher Ayachi
Abdelmottaleb Ben Lamine
Laboratory of Quantum physics LR 18 ES 18,
Faculty of Sciences of Monastir,
Monastir,
Tunisia
E-mail: *kodsphysique@yahoo.fr*

Eder C. Lima
Mariene R. Cunha
Institute of Chemistry,
Federal University of Rio Grande do Sul (UFRGS),
Porto Alegre, RS,
Brazil

HIGHLIGHTS

- We investigated the physical nature of the adsorption of the RR-120 on particles using models based on the formalism of statistical physics.
- Five models were performed and proposed to fit the RR-120 isotherm curves.
- Possible adsorption mechanisms associated with RR-120 were theoretically analyzed within the parameters of the statistical physics model.
- This investigation provides detailed information about the stereographic mechanism of the adsorption process.
- The energetic characteristics at each stage are given at the microscopic level.

INTRODUCTION

Environmental pollution has recently become a severe problem worldwide. The synthesis of industrial products such as cosmetics, food and textiles has participated in the formation of wastewater contaminated with dyes. In fact, dyeing a textile loses about 10–60% of reactive dyes, and produces large quantities of colored wastewater (Hessel *et al.* 2007; Cardoso *et al.* 2011).

Dyes are extensively used for industrial, chemical, printing, cosmetic use, and clinical purposes as well as textile dyeing because of their chemical stability; however, they cause serious environmental and health problems and are not biodegradable (Srinivasan & Viraraghavan 2010; Eren 2012). It has been demonstrated that most of these dyes can cause several allergies, skin irritation (Brookstein 2009)

doi: 10.2166/wst.2020.347

cancer proliferation (Carneiro *et al.* 2010), and mutation in humans (de Lima *et al.* 2007; Carneiro *et al.* 2010). Their presence at even low concentrations can be an obstacle to the use and reuse of water.

Reactive dyes are typically azo-based chromophores combined with different types of reactive groups (Dias *et al.* 2003). These complex molecular structures make them very difficult to be removed from wastewaters (Allege *et al.* 2016). Among reactive dyes in the textile industry, Reactive Red 120 (RR-120) is one of the frequently used ones. Recently, great scientific attention has been paid to remove dyes from wastewaters not only due to their toxicity but also because of their visibility. Adsorption, coagulation, advanced oxidation, and photodegradation (Naushad *et al.* 2019a) are some commonly used methods. With low capital investment cost, the adsorption process is one of the most commonly employed techniques for the extraction of synthetic dyes from aqueous effluents (Ozcan & Ozcan 2005; Machado *et al.* 2011; Mosallanejad & Arami 2012; Somasekhara *et al.* 2012; Vargas *et al.* 2012).

Several low-cost materials are used for the removal of different dyes, such as arginine-modified activated carbon (Naushad *et al.* 2019b), nano-sized chitosan blended polyvinyl alcohol (Anitha *et al.* 2016), eggshell (Rápó *et al.* 2020) and composite sorbent coated with siderite nanoparticles (Alshammari *et al.* 2020). However, activated carbon is found in large quantities and it is easy to use, in addition to being low cost.

The carbon-based materials are the most used adsorbents to remove water pollutants like dyes. The adsorption capacity of this type of adsorbents could change by many orders of magnitude, depending on its preparation conditions (Tan *et al.* 2008; Umpierres *et al.* 2018; Lima *et al.* 2019). In general terms, activated carbons must be thought of as being the most effective adsorbents. Their performance in removing from water contaminants such as metals, rare earth elements, phenolic and aromatic derivatives (including dyes and pesticides), pharmaceuticals, and drugs has been reported (Haghseresht *et al.* 2002; Dąbrowski *et al.* 2005).

Calvete *et al.* (2009) have achieved the RR-120 adsorption on the Brazilian pine-fruit shell activated carbon. The equilibrium adsorbed quantities as a function of RR-120 concentration were determined and modeled empirically at 298 K. The experiment was achieved in order to evaluate the adsorption capacity of activated carbon as a function of the environment change (at 303, 308, 313, 318 and 323 K).

The objective of this work is to investigate the physical nature of the adsorption of RR-120 on particles using models based on the formalism of statistical physics. The five models were performed and proposed to fit the RR-120 isotherms curves. The fitting process was achieved in the ideal gas law approximation and the approach of the law of real gas interactions. The possible adsorption mechanisms associated with this dye (RR-120) and tested adsorbents were theoretically analyzed via the interpretation of the parameters of the statistical physics model. The novelty of this investigation is to provide detailed information about the stereographic mechanism of the adsorption process through the fitted parameter values of the used models. The energetic characteristics of the stages of the process are given at a microscopic level as well as global thermodynamic potentials.

MATERIALS AND METHODS

Activated carbon

The Brazilian pine-fruit (piñon) shell was dried and milled, as previously reported (Calvete *et al.* 2009). The carbonization of the Brazilian pine-fruit shells was achieved by adding 20.0 g of milled shell and 50.0 mL of concentrated sulfuric acid (98% weight, 1.98 $g \cdot mL^{-1}$) in a 1 L glass beaker to produce a black carbonaceous residue. This solid material was magnetically stirred for 15 minutes and combined with 350 mL of water. The system was then heated to 373 K and kept at this temperature for 2 hours under magnetic agitation. Afterward, the non-activated carbonized Brazilian pine-fruit shell was filtered, washed with water and then with 1.0 mol L^{-1} of K_2CO_3 solution, followed by extensive washing with water until the washing liquids reached pH 6.0. The carbonized pine waste was then dried at 423 K for 2 hours and kept in a desiccator. The yield of this carbonization step was 70%.

A chemical and physical activation method was followed. An amount of 10.0 g of previously non-activated carbonized material was placed in a quartz reactor provided with a gas inlet and outlet, which was then placed in a vertical cylindrical furnace to activate the carbon material. The system was heated up to 1,123 K, at a heating rate of 7 $K \cdot min^{-1}$ under N_2 atmosphere (flow rate: 100 $mL \cdot min^{-1}$). Secondly, the temperature was kept isothermal for 1.5 h, and the gas flow was switched to CO_2 (flow rate: 150 $mL \cdot min^{-1}$). Afterward, the system was cooled down to room temperature for 2 h, and the gas was again switched

to N_2. The chemically and physically activated carbon obtained was further ground in a disk mill, followed by sieving, obtaining an adsorbent with a particle size lower than 53 μm. The chemically and physically activated carbon obtained was assigned as CPAC. The yield of this activation process was 45%. Considering the earlier carbonization step carried out with sulfuric acid, the total yield for CPAC adsorbent was 32%.

Considering that this paper focuses on the statistical physics models, the characterization of the activated carbon is presented in the Supplementary Material.

RR-120 molecule

The RR-120 dye belongs to the large family of azo dyes, which are characterized by the presence of the azo group (-N=N-). It also belongs to the large family of reactive dyes which owe their name to the presence of the reactive chemical function of triazine or vinylsulfone type. Figure 1 shows the chemical structure of RR-120 (Calvete *et al.* 2009). The solubility in water is ensured by the multiple sulfonate groups which account for the anionic molecules in aqueous media. The deionized water was used to prepare the solutions of RR-120, which was purchased from Sigma Aldrich as a commercially textile dye with 80% dye content and was used without further purification. RR-120 has six sulfonate groups in highly acidic solution, so the main characteristic structural features of a typical reactive dye molecule are (Calvete *et al.* 2009):

- the reactive system, enabling the dye to form covalent bonds between the dye and the cotton fiber;
- the chromophoric group;
- a bridging group that links the reactive system to the chromophore;
- solubilising groups that make the dye soluble in water (Calvete *et al.* 2009).

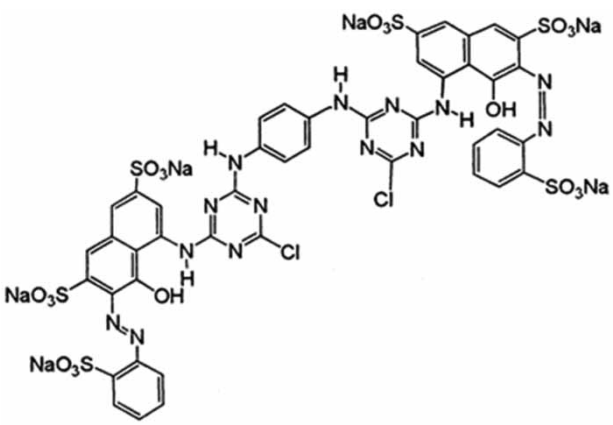

Figure 1 | Chemical structure of RR-120 dye molecule.

Some adsorption experiments have been carried out to evaluate the removal of RR-120 by using the activated carbon as adsorbent (Calvete *et al.* 2009):

- 50.0 mg of adsorbent was put in 50 mL cylindrical polypropylene flasks containing 20.0 mL of the dye solutions (50.00–1,200.0 $mg{\cdot}L^{-1}$).
- The mixture was agitated for 3 h using an acclimatized shaker at temperatures ranging from 298 to 323 K to attain the equilibrium.
- After the batch contact, the slurries were centrifuged at 3,600 rpm for 5 minutes to separate the solid adsorbent from the remaining dye solution.
- After aliquots of dye solution were properly diluted from 1 to 10 mL into volumetric flasks of 50–100 mL, concentrations of this dye solution were determined by visible spectrophotometry at 534 nm, using a Fenton 600 S spectrophotometer.

The main results are summarized in Figure 2. The adsorption capacity was calculated by the following Equation (1):

$$Q = \frac{(c_i - c_e)}{m} V \tag{1}$$

where Q ($mg{\cdot}g^{-1}$) is the dye adsorbed mass (mg) per the adsorbent mass (g), c_i and c_e are respectively the initial dye concentration ($mg{\cdot}L^{-1}$) and the final dye concentration ($mg{\cdot}L^{-1}$), V is the dye solution volume (L), and m is the adsorbent mass (g).

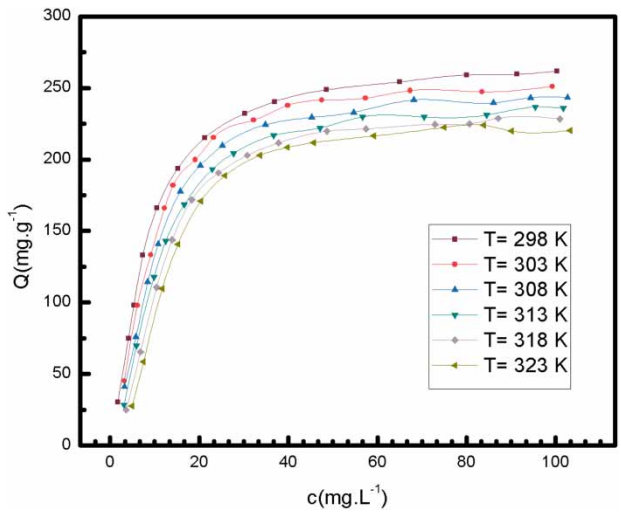

Figure 2 | Adsorption isotherms of RR-120 dye on active carbon at six temperatures.

THEORY: ADSORPTION DOUBLE LAYER WITH ONE ENERGY

In the following, we use the statistical formalization to get the adsorption model. We give an analytical expression of the double layer with one energy. The reaction of adsorption between dye molecules D on one receptor site S can be written as the following Equation (2) (Ayachi *et al.* 2018):

$$nD + S = D_nS \tag{2}$$

where n is the number of molecules adsorbed per site, D is the molecule, S is the receptor site, and D_nS is the formed complex on the site.

In order to model the phenomenon of adsorption, the grand-canonical ensemble is adopted. This ensemble is suitable for the study of systems in contact with a reservoir of heat and particles: the energy and the number of particles of the system are variable, their average values being identified with the corresponding thermodynamic quantities. The grand-canonical partition function is written (Ayachi *et al.* 2018) by Equation (3):

$$Z_{gc} = \sum_{N_i} e^{-\beta(-\varepsilon-\mu)N_i} \tag{3}$$

where $\beta = 1/(K_BT)$ is the Boltzmann factor, T is the temperature, K_B is the Boltzmann constant, μ is the chemical potential, N_i is the site occupancy number and $(-\varepsilon)$ is the adsorption energy of the site with $\varepsilon > 0$.

The grand-canonical partition function for a receiver site in the case of a double adsorption layer with one energy (Sellaoui *et al.* 2016) is written as Equation (4):

$$z_{gc} = 1 + e^{\beta(\varepsilon+\mu)} + e^{2\beta(\varepsilon+\mu)} \tag{4}$$

The grand-canonical partition function for N_m receptor sites is given in Equation (5) (Sellaoui *et al.* 2016):

$$Z_{gc} = (z_{gc})^{N_m} \tag{5}$$

The average number of occupancy of one site is given by Equation (6) (Sellaoui *et al.* 2016):

$$N_0 = K_BT\frac{\partial}{\partial\mu}(\ln Z_{gc}) = N_mK_BT\frac{\partial}{\partial\mu}(\ln z_{gc}) \tag{6}$$

$$N_0 = N_m\frac{(\frac{c}{C_{1/2}})^n + 2(\frac{c}{C_{1/2}})^{2n}}{1 + (\frac{c}{C_{1/2}})^n + (\frac{c}{C_{1/2}})^{2n}} \tag{7}$$

where c is the concentration of RR-120 dye (mg·L^{-1}), and $C_{1/2}$ is the concentration at half-saturation (mg·L^{-1}).

The adsorbed amount Q (Sellaoui *et al.* 2016) for the double layer model with one energy is written as Equation (8):

$$Q = nN_0 = nN_m\frac{\left(\frac{c}{C_{1/2}}\right)^n + 2\left(\frac{c}{C_{1/2}}\right)^{2n}}{1 + \left(\frac{c}{C_{1/2}}\right)^n + \left(\frac{c}{C_{1/2}}\right)^{2n}} \tag{8}$$

This is the final analytical expression of this model that will be used to describe and interpret the adsorption process in terms of the parameters n, N_m, and $C_{1/2}$. The corresponding partition function and expression from other models proposed to fit the adsorption isotherm are present in Table 1.

When we focus on the previous work (Calvete *et al.* 2009) we notice that the model used for the adsorption isotherm does not have, in its expression, parameters which give information about the adsorption phenomenon on the microscopic scale, namely the distribution of molecules on the surface as well as its adsorption energies. In our work, Equation (8) clearly shows the importance of the statistical physics model since it includes steric and energetic parameters making it possible to clarify the adsorption process at the microscopic level. So, the importance of this paper is to give a physical sense to the adsorption process from the statistical model that the empirical models do not allow.

CHOICE OF THE BEST FITTING MODEL

Now for modeling of our experimental adsorption isotherms, we have to use five statistical physics model expressions. The following five adsorption models were considered: monolayer adsorption at one energy, monolayer adsorption with two horizontal energies, double layer adsorption with one energy, double layer adsorption with two vertical energies and multilayer adsorption with saturation. The best fitting model will be the one that shows a better correlation with the experimental adsorption isotherms. This is expressed by the best values of the R^2 adjustment coefficient (Ayachi *et al.* 2018).

In Table 2, we present the values of the adjustment coefficients for each model given by a computer-assisted modeling analysis. These values of the adjustment coefficients show that the double layer model with one energy is the best fitting model.

Table 1 | Expressions of adsorbed quantity for the proposed models

Statistical physics model	Adsorbed quantity
Monolayer model with one energy: model 1	$Q = n.N_0 = \frac{n.N_m}{1+\left(\frac{C_{1/2}}{c}\right)^n}$
Monolayer model with two energies: model 2	$Q = \frac{n_1 N_{1m}}{1+\left(\frac{c_1}{c}\right)^{n_1}} + \frac{n_2 N_{2m}}{1+\left(\frac{c_2}{c}\right)^{n_2}}$
Double layer model with one energy: model 3	$Q = nN_m \frac{\left(\frac{c}{C_{1/2}}\right)^n + 2\left(\frac{c}{C_{1/2}}\right)^{2n}}{1+\left(\frac{c}{C_{1/2}}\right)^n + \left(\frac{c}{C_{1/2}}\right)^{2n}}$
Double layer with two energies: model 4	$Q = nN_m \frac{\left(\frac{c}{C_1}\right)^n + 2\left(\frac{c}{C_2}\right)^{2n}}{1+\left(\frac{c}{C_1}\right)^n + \left(\frac{c}{C_2}\right)^{2n}}$
Multilayer with saturation: model 5	$Q = \frac{nN_m[F_1(c)+F_2(c)+F_3(c)+F_4(c)]}{G(c)}$
	$F_1(c) = \frac{-2\left(\frac{c}{c_1}\right)^{2n}}{1-\left(\frac{c}{c_1}\right)^n} + \frac{\left(\frac{c}{c_1}\right)^n\left(1-\left(\frac{c}{c_1}\right)^{2n}\right)}{\left(1-\left(\frac{c}{c_1}\right)^n\right)^2}$
	$F_2(c) = \frac{2\left(\frac{c}{c_1}\right)^n\left(\frac{c}{c_2}\right)^n\left(1-\left(\frac{c}{c_2}\right)^{N_2 n}\right)}{1-\left(\frac{c}{c_2}\right)^n}$
	$F_3(c) = \frac{-N_2\left(\frac{c}{c_1}\right)^n\left(\frac{c}{c_2}\right)^n\left(\frac{c}{c_2}\right)^{N_2 n}}{1-\left(\frac{c}{c_2}\right)^n}$
	$F_4(c) = \frac{\left(\frac{c}{c_1}\right)^n\left(\frac{c}{c_2}\right)^{2n}\left(1-\left(\frac{c}{c_2}\right)^{N_2 n}\right)}{\left(1-\left(\frac{c}{c_2}\right)^n\right)^2}$
	$G(c) = \frac{1-\left(\frac{c}{c_1}\right)^{2n}}{1-\left(\frac{c}{c_1}\right)^n} + \frac{\left(\frac{c}{c_1}\right)^n\left(\frac{c}{c_2}\right)^n\left(1-\left(\frac{c}{c_2}\right)^{N_2 n}\right)}{1-\left(\frac{c}{c_2}\right)^n}$

The effect of temperature on the number of adsorbed molecules per site

We can clearly understand from Equation (2), which is the adsorption reaction, that n is the stoichiometric coefficient of this equation. Nevertheless, this number of adsorbed molecules per site, n, can also be considered as a steric parameter. The role of the previously mentioned number is to give information about the geometrical properties of the adsorbed molecules on the adsorption surface: that is to say, on the topography of the adsorbed molecule (Khalfaoui *et al.* 2012).

Table 2 | Calculated values of the adjustment coefficient R^2 for the five used model expressions

T (K)	Monolayer adsorption at one energy	Monolayer adsorption with two energies	Double-layer adsorption at one energy	Double-layer adsorption with two energies	Multilayer adsorption with saturation
298	0.99934	0.99909	0.99945	0.9994	0.99919
303	0.99893	0.99863	0.9989	0.99882	0.99869
308	0.99893	0.99935	0.99916	0.99916	0.99865
313	0.99955	0.9994	0.99951	0.99951	0.99945
318	0.99965	0.9997	0.99975	0.99972	0.99958
323	0.99951	0.26794	0.99947	0.99946	0.9994

The linking of the molecule at the receptor site can be achieved through two ways, but that depends on its geometry as well as the angle of incidence on the adsorption surface: perpendicular and parallel anchoring. Parallel anchoring occurs if the number n of adsorbed molecules per site is greater than or equal to unity. In this case, the site is occupied by a portion of the molecules. In this respect, Figure 3 shows the number of adsorbed molecules of the RR-120 dye per receptor site of the adsorbent and for each temperature.

It is worth noting that whatever the value of the temperature, n is greater than 1. This number varies between 1.06 and 1.67. It is essential to mention that n is a decimal number. This can be justified by the fact that these values are averages between plenty of anchorages on the sites such as occupied by one dye molecule and the sites occupied by two dye molecules.

We consider the presence of only anchorages by one or two molecules, to be more understandable.

If we symbolize by x, the percentage of sites occupied by one dye molecule of RR-120 and by $(1-x)$ those occupied by two dye molecules of RR-120, for $n = 1.29$, for instance, we can write $1.29 = x.1 + (1-x).2$, which gives a rate of 71% of sites occupied by one molecule of RR-120 dye and a rate of 29% of the occupied sites by two molecules of RR-120 dye.

Table 3 | Effect of temperature on the number of adsorbed dye molecules n

T (K)	n
298	1.07
303	1.20
308	1.26
313	1.29
318	1.48
323	1.67

The values of n for each temperature are presented in Table 3. Along with that, Figure 3 illustrates that a rise in temperature leads to a rise in n. Equation (2) better explains this. It can, indeed, be split into two stages, the aggregation process: $n\mathrm{D} \rightarrow \mathrm{D}_n$ where n dye molecules are gathered; then, this aggregate is anchored on the receptor site: $n\mathrm{D} + \mathrm{S} \rightarrow \mathrm{D}_n\mathrm{S}$. Thus the increase of n with temperature is due to the aggregation process, which is endothermic.

Effect of temperature on the number of sites per unit area N_m

We have found out that the density of the receptor sites gets reduced with temperature: this is a plain effect that concerns thermal agitation causing, in turn, an inhibition of dye molecules anchoring on the receptor sites. Figure 4 represents the reduction of N_m with temperature, while Table 4 provides us with N_m values for every temperature.

ADSORPTION ENERGY

Effect of the temperature on the half-saturation concentration $C_{1/2}$

A clear presentation of the value of the half-saturation concentration for each temperature is embodied in Table 5. This shows that an increase in temperature has led to an increase in the half-saturation concentration. Figure 5 better illustrates these outcomes. However, the next paragraph states that the growth of $C_{1/2}$ has paved the way for a variation in the adsorption energy.

Adsorption energy

The interaction between the RR-120 dye and the activated carbon is characterized by adsorption energy $(-\varepsilon)$. As was

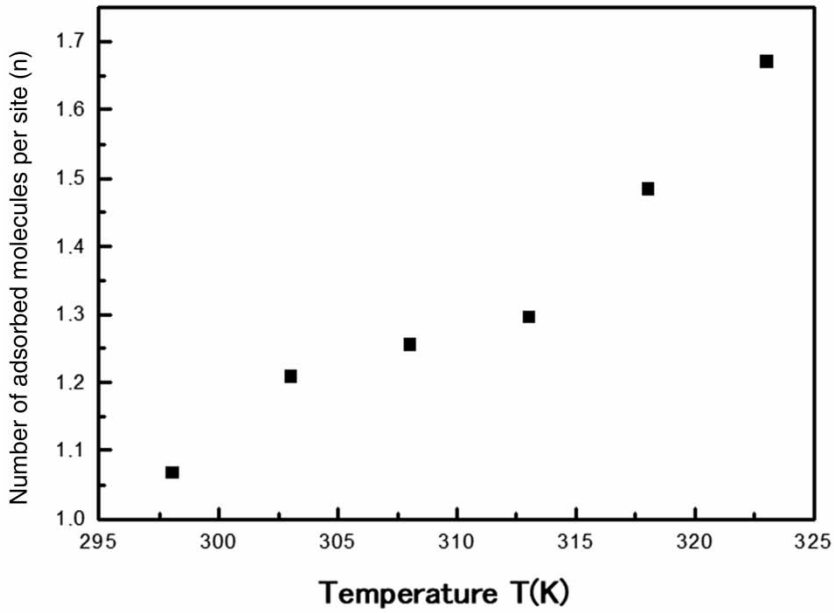

Figure 3 | Variation of n as a function of temperature.

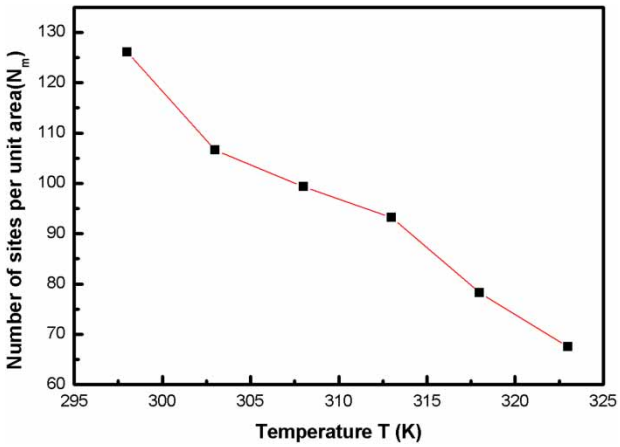

Figure 4 | Variation of N_m as a function of temperature.

Table 4 | Effect of temperature on N_m, the number of sites per unit area

T (K)	N_m (mg/g)
298	126.07
303	106.58
308	99.36
313	93.14
318	78.20
323	67.46

developed previously, the parameter $C_{1/2}$ is highly connected with the adsorption energy ($-\varepsilon$) by the relation given by (Ayachi *et al.* 2018):

$$C_{1/2} = C_S.e^{\frac{\Delta E_a}{K_B T}} \tag{9}$$

C_s stands for the solubility of RR-120, which is 70,000 mg·L $^{-1}$ at ambient temperature, and ΔE_a is the module of the molar adsorption energy (kJ·mol^{-1}).

$$\Delta E_a(\text{kJ} \cdot \text{mol}^{-1}) = RT.\ln\left(\frac{C_S}{C_{1/2}}\right) \tag{10}$$

Looking at Figure 6, we can notice clearly the variation of the adsorption energy with the temperature. By realizing that the values of the adsorption energy are positive in modulus, this can signal the exothermicity of the adsorption reaction, which will be verified by the study of the internal energy in the next section. One other thing worth noting is that the adsorption energy values are unable to exceed 40 kJ·mol^{-1}. That leads us to deduce that the adsorption is physisorption. Thus, the structure of the RR-120 cannot be subject to modification. It is clear that the boost in temperature goes hand in hand with a boost in the adsorption energy proving the influence of temperature on the environment of the adsorbate.

Table 5 | Effect of the temperature on the half-saturation concentration $C_{1/2}$

T (K)	$C_{1/2}$ (mg·L^{-1})
298	7.73
303	8.46
308	9.26
313	10.13
318	10.94
323	12.06

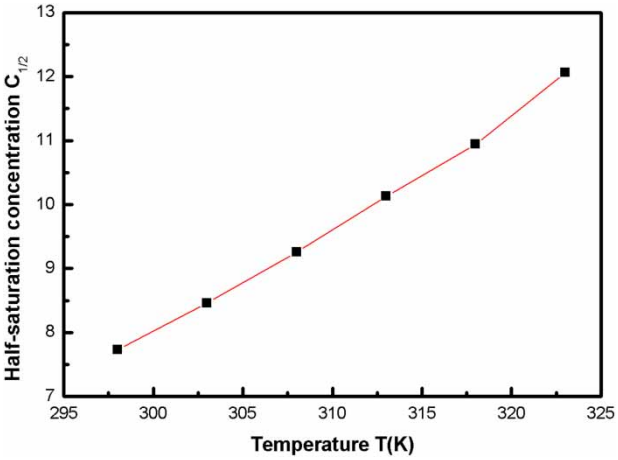

Figure 5 | Variation of $C_{1/2}$ as a function of temperature.

INTERNAL ENERGY

The internal energy, E_{int}, can be expressed by (Ben Manaa *et al.* 2018):

$$E_{\text{int}} = -\frac{\partial(\ln Z_{gc})}{\partial\beta} + \frac{\mu}{\beta}.\frac{\partial(\ln Z_{gc})}{\partial\mu} \tag{11}$$

where μ is chemical potential for the real gas (kJ).

With the adopted model for the description of the adsorption process, the internal energy will have the expression given by:

$$E_{\text{int}} = K_B T.nN_m.\frac{\left(\frac{c}{C_{1/2}}\right)^n + 2\left(\frac{c}{C_{1/2}}\right)^{2n}}{1+\left(\frac{c}{C_{1/2}}\right)^n + \left(\frac{c}{C_{1/2}}\right)^{2n}}\ln\left(\frac{C_{1/2}}{z_{tr}}\right) \tag{12}$$

where z_{tr} is the translation partition function per unit volume.

To understand any adsorption phenomenon, we need to introduce the energy concept. Looking at Figure 7, we can notice clearly the variation of the internal energy with the temperature.

It has been proved that internal energy keeps the same pace and is always negative. Hence there is an energy release, and this is how the spontaneity as well as exothermicity of the phenomenon is proved. As long as the adsorption

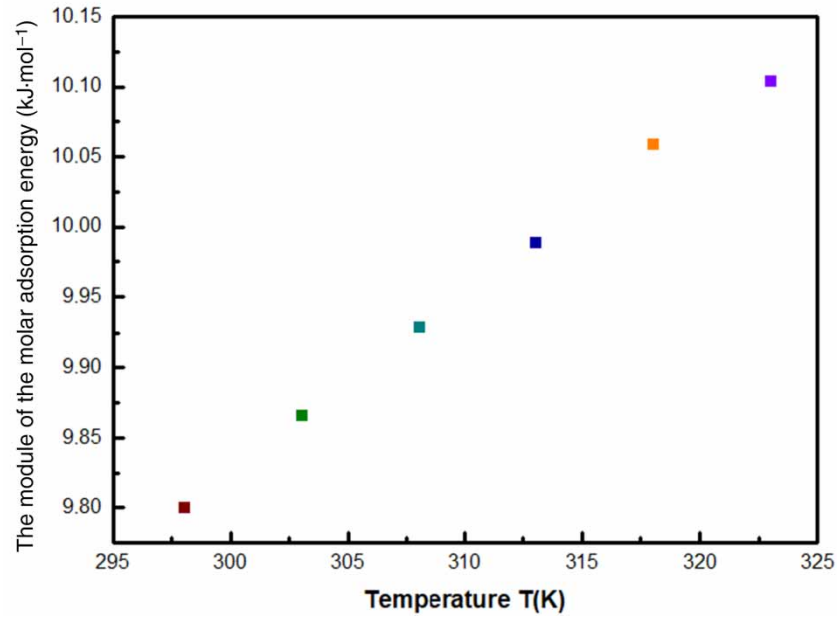

Figure 6 | Variation of the module of the molar adsorption energy ΔE_a with temperature.

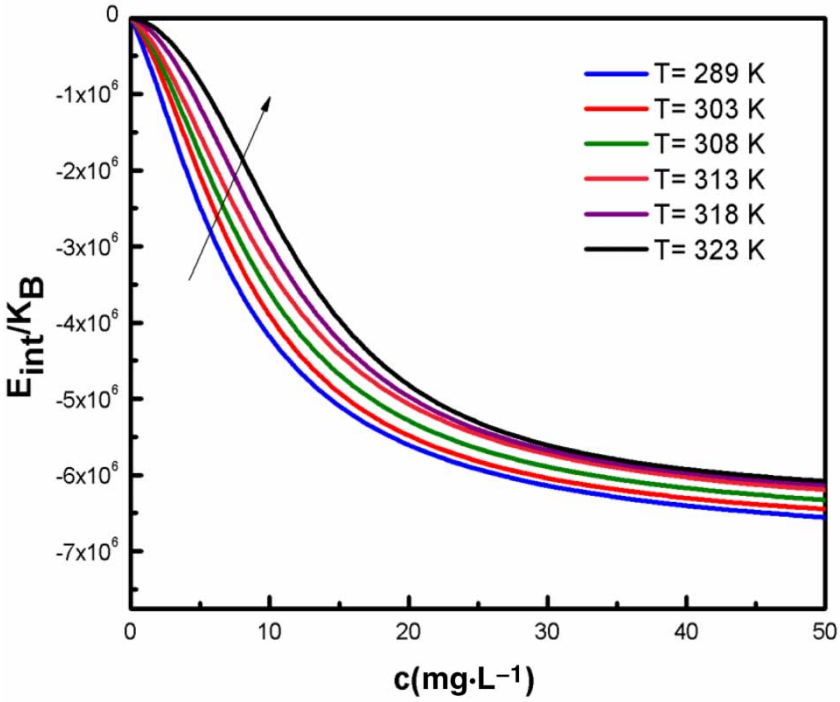

Figure 7 | Variation of internal energy E_{int} with concentration.

of the RR-120 dye on the activated carbon is physisorption, the previously mentioned result remains predictable and expected. In fact, what explains well the increase of internal energy in absolute value with the concentration is the increase of adsorbed quantity. Added to that, we should mention that the increase of the adsorption energy leads systematically to the increase in absolute values.

STUDY OF THE FREE ENTHALPY

Information about adsorption phenomena spontaneity can be given through the free enthalpy.

$$G = \mu Q \tag{13}$$

It is possible, so, to drift the free enthalpy thanks to the best fitting model of isotherm curves. This will be expressed this way:

$$G = K_B T n N_m . \ln\left(\frac{c}{z_{tr}}\right) . \frac{\left(\frac{c}{C_{1/2}}\right)^n + 2\left(\frac{c}{C_{1/2}}\right)^{2n}}{1 + \left(\frac{c}{C_{1/2}}\right)^n + \left(\frac{c}{C_{1/2}}\right)^{2n}} \tag{14}$$

Looking at Figure 8, we can notice undoubtedly the variation of the free enthalpy with the temperature. Either from zero or all other temperature degrees, the free enthalpy gets reduced algebraically. Nevertheless, we should bear in our minds that the absolute value of the free enthalpy increases with the concentration. As soon as the adsorption process is set in motion, we become able to notice that the receptor sites are vacant, proving the way to an easy molecule retention.

Getting close to a saturation status and through the high concentration rate, RR-120 dye molecules are by no means able to reach the receptor sites of activated carbon since they are all occupied. In this respect, we can conclude from the figure that the increase of temperature obviously results in a rise in the free enthalpy. At this point, the system becomes clearly more stable. More than this, the spontaneity of the RR-120 dye adsorption on activated carbon is proved by the negative value of the free enthalpy.

STUDY OF ENTROPY

Entropy S is a quantity that measures the disorder of a system at a microscopic level. The entropy is given by (Ben Manaa *et al.* 2018):

$$\frac{S}{K_B} = \ln(Z_{gc}) - \beta \frac{\partial(\ln Z_{gc})}{\partial \beta} \tag{15}$$

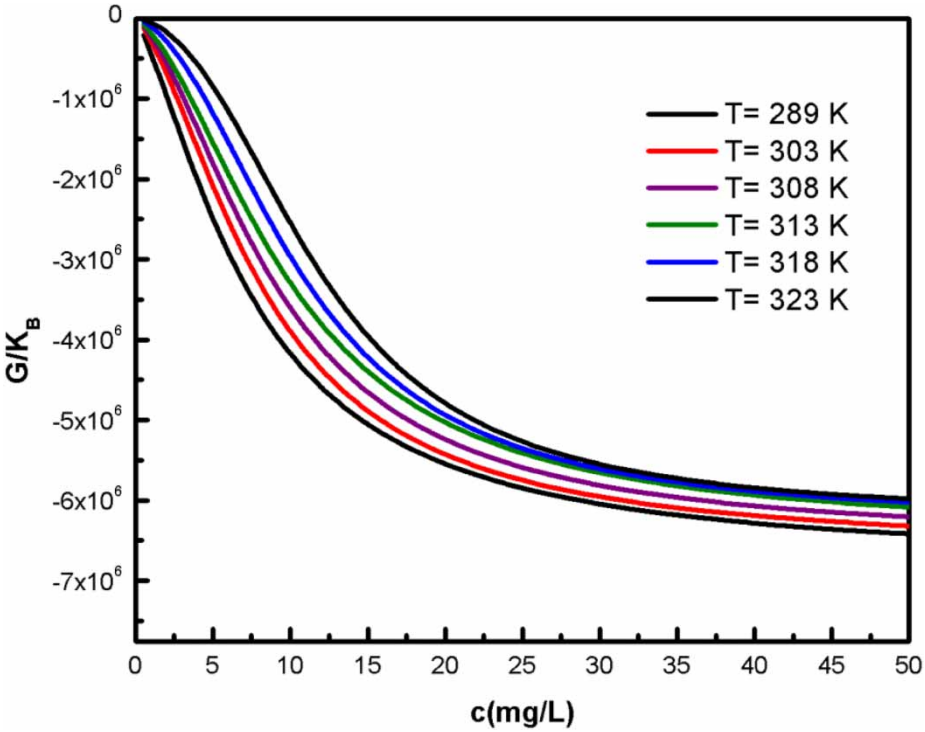

Figure 8 | Variation of free enthalpy *G* with concentration.

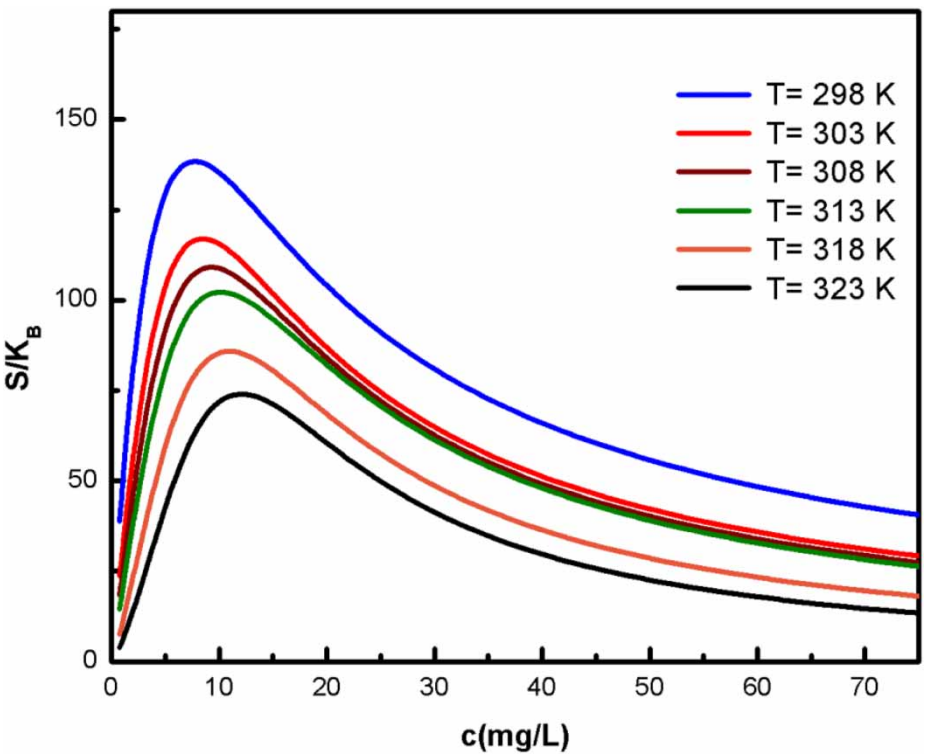

Figure 9 | Variation of entropy *S* with concentration.

With the best fitting model adopted for a description of the adsorption process, the entropy will have the expression:

$$\frac{S}{K_B} = N_m \left[\ln\left(1 + \left(\frac{c}{C_{1/2}}\right)^n + \left(\frac{c}{C_{1/2}}\right)^{2n}\right) - \frac{\left(\frac{c}{C_{1/2}}\right)^n \ln\left(\left(\frac{c}{C_{1/2}}\right)^n\right) + \left(\frac{c}{C_{1/2}}\right)^{2n} \ln\left(\left(\frac{c}{C_{1/2}}\right)^{2n}\right)}{1 + \left(\frac{c}{C_{1/2}}\right)^n + \left(\frac{c}{C_{1/2}}\right)^{2n}} \right] \quad (16)$$

Figure 9 illustrates the variation of entropy as a function of temperature. When concentration reaches a low degree (i.e., for concentration levels which are below the half-saturation concentration), we may notice that the receptor sites remain empty; the RR-120 dye molecules have a diversity of receptor sites to choose to give a more significant room for the disorder to increase. Hence, we can understand why the entropy, along with the concentration, has risen at first. When the surface of activated carbon tends to be saturated, the disorder lessens. This occurs after the half-saturation. By doing so, the entropy lowers, with a high possibility of becoming zero.

CONCLUSION

This work allowed us to present the analytical models developed by the formalism of statistical physics. An attempt has been made to model the adsorption isotherms of the dye RR-120 on activated carbon. The double layer model with one energy is the best fitting model. This model has allowed us to achieve the following results. Steric and energetic interpretations were performed. The adsorption of RR-120 on activated carbon is of the physisorption type, as confirmed by the adsorbed energy values and it is exothermic as verified by the internal energy. The free enthalpy has negative values, whatever the temperature, which demonstrated the spontaneity of the phenomenon. The monitoring of the disorder of the system was realized through the study of entropy.

ACKNOWLEDGEMENTS

The authors thank the Foundation for Research Support of the State of Rio Grande do Sul (FAPERGS), National Council for Scientific and Technological Development (CNPq, Brazil), and Coordination of Improvement of Higher Education Personnel (CAPES, Brazil) for financial support and sponsorship. Authors are grateful to Nanoscience and Nanotechnology Center (CNANO-UFRGS), and Microscopy and Microanalysis Center (CME-UFRGS) of Federal University of Rio Grande do Sul (UFRGS). We are also grateful to ChemAxon for giving us an academic research license for the Marvin Sketch software, Version 20.3 (http://www.chemaxon.com), used for molecule physical–chemical properties.

DATA AVAILABILITY STATEMENT

All relevant data are included in the paper or its Supplementary Information.

REFERENCES

Allege, C., Moulin, P., Maisseu, M. F. & Charbit, M. F. 2016 Treatment and reuse of reactive dyeing effluents. *J. Membr. Sci.* **269**, 15–34.

Alshammari, M., Al Juboury, M. F., Naji, L. A., Faisal, A. A. H., Zhu, H., Al-Ansari, N. & Naushad, M. 2020 Synthesis of a novel composite sorbent coated with siderite nanoparticles and its application for remediation of water contaminated with Congo Red Dye. *Int. J. Environ. Res. Public Health* **14**, 177–191.

Anitha, T., Senthil Kumar, P. & Sathish Kumar, K. 2016 Synthesis of nano-sized chitosan blended polyvinyl alcohol for the removal of Eosin Yellow dye from aqueous solution. *J. Water Process Eng.* **13**, 127–136.

Ayachi, F., Lima, E. C., Sakly, A., Mejri, H. & Ben Lamine, A. 2018 Modeling of adsorption isotherms or reactive red RR-120 on *Spirulina platensis* by statistical physics formalism involving interaction effect between adsorbate molecules. *Prog. Biophys. Mol. Biol.* **141**, 47–59.

Ben Manaa, M., Bouaziz, N., Schmaltz, B., Tran Van, F. & Ben Lamine, A. 2018 Study of the effect of variation in temperature and pH on the adsorption process of natural Gardenia yellow dye into TiO_2 mesoporous for dye-sensitized solar cells using the statistical physics formalism: physicochemical and thermodynamic investigation. *Micropor. Mesopor. Mat* **270**, 82–92.

Brookstein, D. S. 2009 Factors associated with textile pattern dermatitis caused by contact allergy to dyes, finishes, foams, and preservatives. *Dermatol. Clinics* **27**, 309–322.

Calvete, T., Lima, E. C., Cardoso, N. F., Dias, S. L. P. & Pavan, F. A. 2009 Application of carbon adsorbents prepared from the Brazilian-pine fruit shell for removal of Procion Red MX 3B from aqueous solution – kinetic, equilibrium, and thermodynamic studies. *Chem. Eng. J.* **155**, 627–636.

Cardoso, N. F., Lima, E. C., Pinto, I. S., Amavisca, C. V., Royer, B., Pinto, R. B., Alencar, W. S. & Pereira, S. F. P. 2011 Application of cupuassu shell as biosorbentfor the removal of textile dyes from aqueous solution. *J. Environ. Manage.* **92**, 1237–1247.

Carneiro, P. A., Umbuzeiro, G. A., Oliveira, D. P. & Zanoni, M. V. B. 2010 Assessment of water contamination caused by a mutagenic textile effluent/dyehouse effluent bearing disperse dyes. *J. Hazard. Mater.* **174**, 694–699.

Dąbrowski, A., Podkościelny, P., Hubicki, Z. & Barczak, M. 2005 Adsorption of phenolic compounds by activated carbon – a critical review. *Chemosphere* **58** (8), 1049–1070.

de Lima, R. O. A., Bazo, A. P., Salvadori, D. M. F., Rech, C. M., Oliveira, D. P. & Umbuzeiro, G. A. 2007 Mutagenic and carcinogenic potential of a textile azo dye processing plant effluent that impacts a drinking water source. *Mutat. Res. Genet. Toxicol Environ. Mutagen.* **626**, 53–60.

Dias, A. A., Bezerra, M. R., Lemos, M. P. & Pereira, N. A. 2003 In vivo and lacasse catalyzed decolorization of xenobiotic azo dyes by a basidiomycetous fungus: characterization of its ligninolytic system. *World J. Microbiol. Biotechnol.* **19**, 969–975.

Eren, Z. 2012 Ultrasound as a basic and auxiliary process for dye remediation: a review. *J. Environ. Manage.* **104**, 127–141.

Haghseresht, F., Nouri, S., Finnerty, J. J. & Lu, G. Q. 2002 Effects of surface chemistry on aromatic compound adsorption from dilute aqueous solutions by activated carbon. *J. Phys. Chem. B* **106**, 10935–10943.

Hessel, C., Allegre, C., Maisseu, M., Charbit, F. & Moulin, P. 2007 Guidelines and legislation for dye house effluents. *J. Environ. Manage.* **83**, 171–180.

Khalfaoui, M., Nakhli, A., Knani, S., Baouab, H. V. & Ben Lamine, A. 2012 On the statistical physics modeling of dye adsorption onto anionized nylon: consequent new interpretations. *J. Appl. Polym.* **125**, 1091–1102.

Lima, D. R., Gomes, A. A., Lima, E. C., Umpierres, C. S., Thue, P. S., Panzenhagen, J. C. P., Dotto, G. L., El-Chaghaby, G. A. & de Alencar, W. S. 2019 Evaluation of efficiency and selectivity in the sorption process assisted by chemometric approaches: removal of emerging contaminants from water. *Spectrochim. Acta Part A* **218**, 366–373.

Machado, F. M., Bergmann, C. P., Fernandes, T. H. M., Lima, E. C., Royer, B., Calvete, T. & Fagan, S. B. 2011 Adsorption of Reactive Red M-2BE dye from water solutions by multi-walled carbon nanotubes and activated carbon. *J. Hazard. Mater.* **192**, 1122–1131.

Mosallanejad, N. & Arami, A. 2012 Kinetics, and isotherm of sunset yellow dye adsorption on cadmium sulfide nanoparticle loaded on activated carbon. *J. Chem. Health Risk* **2** (1), 31–40.

Naushad, M., Sharma, G. & Alothman, Z. A. 2019a Photodegradation of toxic dye using Gum Arabic-crosslinked-poly(acrylamide)/Ni(OH)$_2$/FeOOH nanocomposites hydrogel. *J. Cleaner Prod.* **241**, 118263. https://doi.org/10.1016/j.jclepro.2019.118263.

Naushad, M., Alqadami, A. A., AlOthman, Z. A., HotanAlsohaimi, I., Algamdi, M. S. & Aldawsari, A. M. 2019b Adsorption kinetics, isotherm and reusability studies for the removal of cationic dye from aqueous medium using arginine modified activated carbon. *J. Mol. Liq.* **293**, 111442. https://doi.org/10.1016/j.molliq.2019.111442.

Ozcan, A. & Ozcan, A. S. 2005 Adsorption of Acid Red 57 from aqueous solutions onto surfactant-modified sepiolite. *J. Hazard. Mater.* **125**, 252–259.

Rápó, E., Előd Aradi, L., Szabó, Á., Posta, K., Szép, R. & Tonk, S. 2020 Adsorption of remazol brilliant violet-5R textile dye from aqueous solutions by using eggshell waste biosorbent. *Sci. Rep.* **10** (1), 1–12.

Sellaoui, L., Knani, S., Erto, A., Hachicha, M. & Ben Lamine, A. 2016 Equilibrium isotherm simulation of tetrachlorethylene on activated carbon using the double-layer model with two energies: steric and energetic interpretations. *Fluid Phase Equilib.* **408**, 259–264.

Somasekhara, R. M. C., Sivaramakrishna, L. & Varada, R. A. 2012 The use of agricultural waste material, Jujuba seeds for the removal of anionic dye (Congo red) from the aqueous medium. *J. Hazard. Mater.* **203**, 118–127.

Srinivasan, A. & Viraraghavan, T. 2010 Decolorization of dye wastewaters by biosorbents: a review. *J. Environ. Manage.* **91**, 1915–1929.

Tan, I. A. W., Ahmad, A. L. & Hameed, B. H. 2008 Adsorption of basic dye on high-surface-area activated carbon prepared from coconut husk: equilibrium, kinetic and thermodynamic studies. *J. Hazard. Mater.* **154**, 337–346.

Umpierres, C. S., Thue, P. S., Lima, E. C., dos Reis, G. S., de Brum, I. A. S., de Alencar, W. S., Dias, S. L. P. & Dotto, G. L. 2018 Microwave activated carbons from Tucumã (*Astrocaryum aculeatum*) seed for efficient removal of 2-nitrophenol from aqueous solutions. *Environ. Technol.* **39**, 1173–1187.

Vargas, A. M. M., Cazetta, A. L., Martins, A. C., Moraes, J. C. G., Garcia, E. E., Gauze, G. F., Costa, W. F. & Almeida, V. C. 2012 Kinetic and equilibrium studies: adsorption of food dyes Acid Yellow 6 Acid Yellow 23, and Acid Red 18 on activated carbon from flamboyant pods. *Chem. Eng. J.* **181**, 243–250.

First received 20 March 2020; accepted in revised form 15 July 2020. Available online 29 July 2020